Colloid & Polymer Sci. **252**, 249–256 (1974)

From the Chemistry Department, N.E. London Polytechnic, London (England)

Studies on recrystallised aluminium hydroxide precipitates

Kinetics and mechanism of dissolution by sodium hydroxide solutions

By A. Packter and H. S. Dhillon

With 6 figures and 2 tables

(Received March 5, 1973)

Introduction

Amorphous colloidal aluminium hydroxide precipitates and their recrystallisation products have been studied by many workers; generally, the amorphous gels recrystallise in dilute aqueous alkaline solution to pseudo-boehmites and then to bayerites and/or gibbsites of sub-microscopic particle size (1, 2, 3, 4). *Souza Santos* (5) has classified such colloidal precipitates by their rate of dissolution. Few quantitative studies have been reported on the dissolution process.

This work extends previous studies (4) on the kinetics of dissolution of amorphous aluminium hydroxide gels. These gels were recrystallised under controlled conditions to give gibbsite powders of different particle size (from 0.03–0.45 microns) and the dissolution of dilute suspensions of these powders by well-stirred solutions of sodium hydroxide was studied at 20–65 °C. The variation of reaction rates with initial powder surface area and mean ionic activity and temperature of the reaction solution has been investigated in detail. Reaction mechanisms are suggested.

Experimental

Materials

Gibbsite P 11/2 powder

300 cm^3 of aluminium sulphate solution (0.2 M A.R. material) was mixed rapidly with 300 cm^3 of sodium hydroxide solution (0.6 M A.R. material) and the pH adjusted to pH 11 with slight excess hydroxide. The amorphous aluminium hydroxide precipitate was then recrystallised for 2 h in the supernatant (5). The precipitate was then filtered, washed four times with double-distilled water to remove adsorbed ions and dried three times – by resuspension in dry acetone and filtering; the remaining moisture was removed by outgassing for 24 h at room temperature with a mercury vapour pump.

Gibbsite P 11/8, P 11/48, P 11/360 and P 11/X (powders)

Four other batches of amorphous precipitate were prepared as above and recrystallised for 8, 48, 360 and 1000 h respectively in the supernatant. The precipitates were then washed and dried in the same manner.

The chemical and physical properties of these powders are summarised below:
particle shape; hexagonal platelets ($W_0/l_0 = 0.48$):
particle length (l_0); *P* 11/20.03 μm, *P* 11/8 0.06 μm, *P* 11/48 0.13 μm, *P* 11/360 0.26 μm, *P* 11/*X* 0.45 μm:
chemical analysis; 0.995 $Al(OH)_3$, 0.005 Na_2O, c. 0.0001 SiO_2:
X-ray diffraction; *P* 11/2 c. 0.7 Gibbsite and c. 0.3 Boehmite; others >0.95 Gibbsite, no Bayerite, no Boehmite:
I.R. spectrophotometry; *P* 11/2 0.72 Gibbsite and 0.28 Boehmite; others >0.98 Gibbsite.

Chemical analysis

0.2 g powder was dissolved completely in 3 M hydrochloric acid (100 cm^3) at 95 C. Al^{+++}, Na^+ were determined by standard methods (6, 7).

X-ray diffraction (8)

The X-ray powder diffraction pattern was photographed on a "Philips" 11.4 cm. Powder Camera, using $Co_{K\alpha}$ radiation, Fe filtered. The sample was mounted in a 0.3 mm diameter berylium-glass capillary and rotated continuously during 6 h exposure. The d-spacings were measured and the patterns compared with those given in the "American Society for Testing Materials" X-ray powder data file, 1969.

Infrared spectrophotometry (9)

The dried Gibbsite powder was reground in an agtae mortar to < 2 μm size and dispersed in potassium bromide discs. The spectrum was obtained on an "Infra-Scan" I.R. spectrophotometer against a pure potassium bromide reference disc of the same thickness; the time for scanning from 4000–650 cm^{-1} was 16 min.

Thermogravimetric analysis (10) was by standard methods.

Electron microscopy (11)

10 mg powder (before and after reaction) was dispersed in a drop of butyl phthalate and the paste was diluted 10 × 5 times with amyl acetate. One drop of the diluted dispersion was then pipetted onto a "Formvar" film on a 100 mesh copper grid and the solvent was evaporated off. The grid was then studied with a "Philips" E.M. 75 Electron Microscope. Different fields were photographed; the overall magnification was 20000 ×. 100 particles were studied in three photomicrographs. Crystal lengths (l) and widths (w) were measured as the long and short axes of the Gibbsite platelets; for regular hexagons of side L, l would equal $2L$ while w would equal $\sqrt{3}L$.

Initial average particle lengths (l_0) were estimated from the relation.

$$l_0 = \sqrt{\frac{\sum_0^x n_{j-1,j} l_{j-1,j}^2}{x}} \quad \text{m}$$

where $n_{j-1,j}$ is the number of particles of length l_{j-1} to l_j, x is the total number of particles, $l_{j-1,j} = (l_{j-1} + l_j)/2$.

Initial specific surface areas (S_0) – for two-directional reaction with hexagonal platelets – were estimated from the relation (see eq. [9A], Discussion),

$$S_0 = \frac{4.6}{\varrho} \frac{\sum_0^x n_{j-1,j} l_{j-1,j}}{\sum_0^x n_{j-1,j} l_{j-1,j}^2} \quad \text{m}^2/\text{g}$$

where ϱ is the density of Gibbsite.

Solutions

Sodium hydroxide solutions (of concentration C = 0.25 to 10 M) were prepared from A.R. material in double glass-distilled CO_2 free water. Concentrations were determined by titration against standard hydrochloric acid. Mean ionic activities ($a_\pm$ values) were obtained from *Åckerlofs* work (12).

E.D.T.A.Ate solution (0.01 M), zinc sulphate solution (0.01 M) and acetic acid–ammonium acetate buffer solution (1 M) for Al analysis were prepared from A.R. materials in double-distilled water.

Reaction kinetics

Gibbsite powder (0.8 g weight) was completely redispersed in large excess (100 cm^3) aqueous sodium hydroxide solution in a "Quickfit" flask by vigorous shaking at 1000 vibrations per minute for 15 seconds. The reaction flask was then shaken at 240 vibrations per minute for the reaction proper in a "*Dubnoff*" Shaker–Water Bath (13) thermostatted at ±1 °C.

1 cm^3 reaction solution was withdrawn for chemical analysis after different reaction times. This aliquot volume was diluted to 10 cm^3 and centrifuged at 1000 r.p.m. for five minutes to remove any trace of suspended finely divided powder that would react with the E.D.T.A.Ate solution; 5 cm^3 solution were then withdrawn and analysed for aluminate anion by a modified *Waenninens* method (7). 0.01 M E.D.T.A.Ate solution (5 cm^3) and 1 M acetic acid-ammonium acetate buffer solution (10 cm^3) were added and the solution was heated at 80 °C for 2 min to convert all aluminate to complexed aquo-aluminium cation at pH 4.5; this solution was then cooled and then 95% ethanol (10 cm^3) and 0.001 M dithizone solution (2 cm^3) were added. The excess E.D.T.A.Ate was then back-titrated against 0.01 M zinc sulphate solution from a micro-burette. 1 cm^3 E.D.T.A.Ate solution used $\equiv$ 0.5800 mg $Al(OH)_3$.

The accuracy was 0.2–0.5%. Aluminate concentrations $(W_{sol})_t$ were determined and corrected for volume changes during the run.

In several runs, a series of separate flasks, each containing the same suspension, was used and successive flasks were removed from the bath after different times. The unreacted powder from each flask was washed with distilled water, filtered and dried to constant weight W_t at 100 °C. The physical properties of these powders was studied by the methods described above.

Dissolution

A series of Gibbsite powders were prepared by controlled crystallisation of amorphous aluminium hydroxide precipitates in high pH solution for 2–1000 h; these consisted of hexagonal platelets of initial average particle lengths l_0 from 0.03–0.45 microns and initial specific surface areas S_0 from 5–65 m^2/g. These powders were dispersed in sodiumhydroxide solutions (concentration C = 0.25–10 M) and their dissolution studied at 20 to 65 °C. The suspension concentration was 0.8 g per 100 cm and the hydroxide was in large excess; this eliminated any variation of reaction rate with hydroxide concentration during a run, simplified the kinetics and allowed separate study of the effects of initial powder weight and surface area and hydroxyl ion activity. The shaking rate was 240 vibrations per minute.

Diffusion

The shaking rate was sufficiently high to eliminate any modification of reaction rate by slow diffusion across the diffusion layer adjacent to the powder surface. The use of dilute suspensions also eliminated retarded contact of reaction solution with powder surface due to slow permeability processes (13, 14, 15).

The reaction rates and rate constants measured were then the actual rates of the chemical reactions at the powder crystal surface.

Physical and chemical changes

The powders first rapidly adsorbed one to more than three monolayers of hydroxyl ion and then dissolved to form aluminate anion (13, 16, 17). The solid and reaction solution were analysed after different reaction times.

The solid

Residual weight W_t decreased continuously during the reaction.

Chemical composition. Infra-red spectrophotometry and thermogravimetric analysis indicated that the solid retained the composition $Al(OH)_3$ for over eighty percent reaction; there was no dehydration to AlOOH during prolonged contact with hot hydroxide solution.

Particle size and shape. Some typical results for the reaction of $P\,11/X$ powder with 4 M sodium hydroxide solution at 50 °C are presented in table 1. The average platelet lengths (l_t) and widths (W_t) decreased uniformly during the reaction; the platelet thickness (h) did not change significantly. The Gibbsite particles retained their hexagonal shape for over eighty percent reaction; W_t/l_t ratios were close to $\sqrt{3}/2$ or 0.86. The dissolution was then twodirectional on the six faces of the hexagonal platelets.

Table 1. Reaction of Gibbsite $P11/X$ powder with 4 M sodium hydroxide solution. Platelet lengths etc.

Time (t) (h)	Residual weight fraction (W_t/W_0)	Platelet length (l_t) (μm)	Platelet width (W_t) (μm)	W_t/l_t ratio	l_t/l_0 ratio
0.00	1.000	0.45	0.38	0.84	1.00
0.33	0.732	0.33	0.27	0.83	0.72
0.67	0.560	0.24	0.19	0.81	0.53
1.00	0.396	0.17	0.14	0.82	0.41
1.50	0.236	0.11	0.09	0.83	0.24

The solution

At any time of reaction, the aluminate concentration $(W_{sol})_t$ in solution, expressed in terms of equivalent weight of $Al(OH)_3$, corresponded to the weight loss $\Delta W_t = (W_0 - W_t)$ of Gibbsite The hydroxide concentration remained practically constant during any reaction.

Kinetics

Reaction order

The kinetics of heterogeneous solid-liquid reactions are generally studied by examination of solid remaining after different reaction times. W_t values were conveniently determined by analysis of the reaction solution for $(W_{sol})_t$; then, $W_t = [W_0 - (W_{sol})_t]$.

Completely recrystallised Gibbsite P 11/X

A typical $W_t - t$ plot is presented in fig. 1; $\log W_t/W_0 - t$ plots are presented in figs. 2A, 3, 4.

For over eighty percent of the dissolution, $\log W_t/W_0$ varied linearly with reaction time. That is, at any time

$$\frac{dW}{dt} = -k_w W_t \quad \text{g/h} \qquad [1]$$

where k_w is a first-order rate constant w.r.t. powder weight.

Partly crystallised Gibbsites

Some typical $W_t - t$ plots for reactions with these other materials are presented in fig. 1. For the first twenty percent dissolution, these materials reacted far more rapidly than the completely crystallised material with any hydroxide solution; then, the rate of dissolution slowed down. Generally, these effects were most marked in the more dilute solutions at lower temperatures. $\log W_t/W_0 - t$ plots are presented in figs. 2B, 2C, 3. Over the range of rapid dissolution, $\log W_t/W_0$ varied linearly with reaction time; the above equation then applied. Then, the $\log W_t/W_0 - t$ gradients decreased continuously and might reach similar values to those for reactions with Gibbsite $P11/X$.

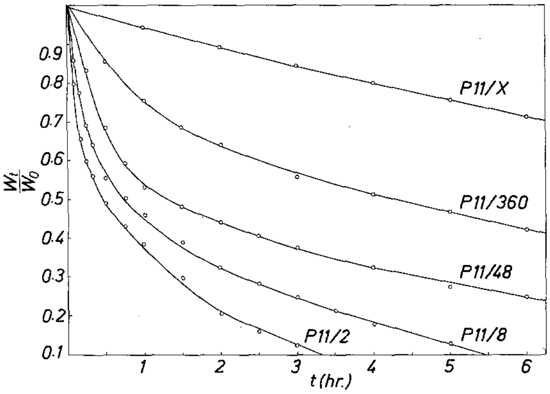

Fig. 1. Dissolution of Gibbsite by sodium hydroxide solution (C = 1 M) at 35 °C. Variation of powder weight with time

Determination of rate constants

For the reactions with Gibbsite $P11/X$, the *rate constants* (k_w) were determined from the gradients of the $\log W_t/W_0 - t$ plots according to the relation,

$$k_w = 2.303 \text{ Grad } [\log W_t/W_0 \text{ v } t \text{ plot}] \;\; h^{-1}. \qquad [3]$$

For the reactions with the other Gibbsites, the *initial rate constants* (k_{w_i}) were determined in the same way from the gradients of the initial linear portions of the $\log W_t/W_0 - t$ plots.

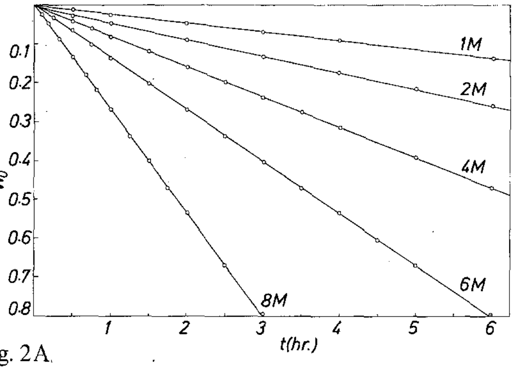

Fig. 2A

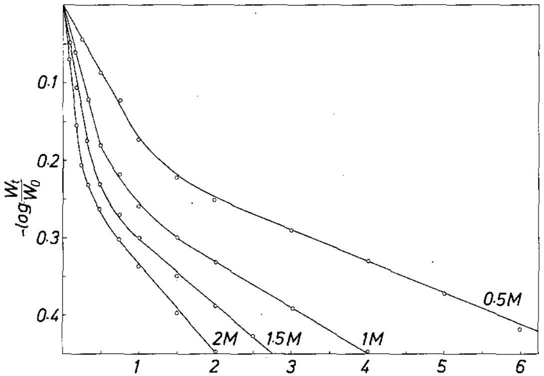

Fig. 2B

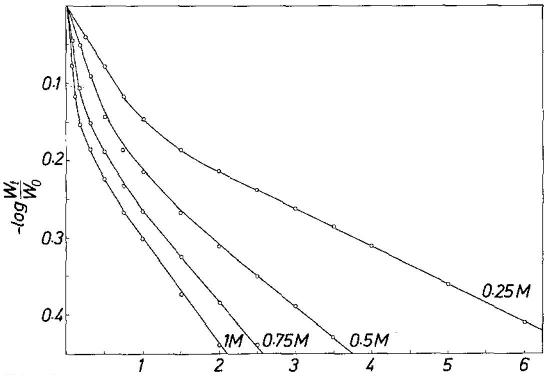

Fig. 2C

Fig. 2A. Dissolution of Gibbsite $P11/X$ by sodium hydroxide solutions at 35 °C. 2B. Dissolution of Gibbsite $P11/48$ by sodium hydroxide solutions at 35 °C. 2C. Dissolution of Gibbsite $P11/2$ by sodium hydroxide solutions at 20 °C. Variation of $\log W_t/W_0$ with time

Half-lifes ($t_{0.5}$) were read off from the whole plots.

Average rate constants ($k_{w_{av}}$) were determined from the half-lifes according to the relation,

$$k_{w_{av}} = \frac{0.69}{t_{0.5}} \quad h^{-1}. \qquad [4]$$

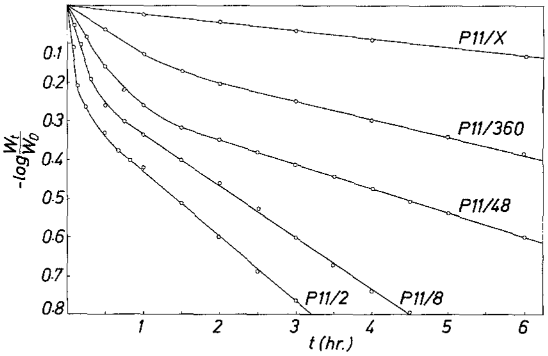

Fig. 3. Dissolution of Gibbsites by sodium hydroxide solution ($C = 1$ M) at 35 °C. Variation of $\log W_t/W_0$ with time

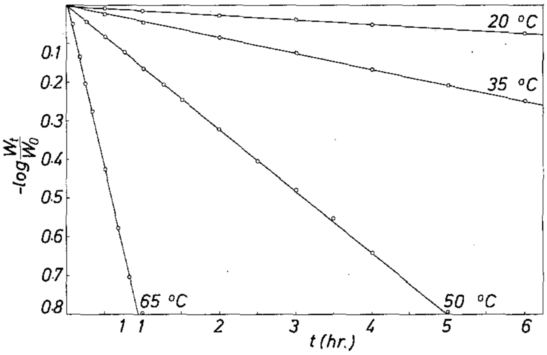

Fig. 4. Dissolution of Gibbsite $P11/X$ by sodium hydroxide solution ($C = 2$M) at different temperatures. Variation of $\log W_t/W_0$ with time

The rate constants for reactions of different Gibbsites with sodium hydroxide solutions of concentrations CM and mean ionic activity $a_\pm$ M are collated in table 2.

Sodium hydroxide concentration

Rates of dissolution at any temperature increased with increasing (excess) hydroxyl ion concentration in the reaction solution. For the reactions with completely crystallised Gibbsite $P11/X$, the rate constant k_w varied linearly with the mean ionic activity $a_\pm$ of the reaction solution upto $a_\pm = 10$ g ion/dm^3; refer to figs. 2A, 5.

Then,

$$k_w = k_{w_1} a_\pm \qquad [5A]$$

where $k_w = k_{w_1}$ at $a_\pm = 1$ g ion/dm^3.

Eq. [1] then becomes more generally,

$$\frac{dW}{dt} = -k_{w_1} W_t a_\pm \quad g/h. \qquad [6]$$

For the rapid dissolution of the partly crystallised Gibbsites, the initial rate constant k_{w_i} varied

Table 2. Rate constants k_w (h^{-1}) and half-lifes $t_{0.5}$ (h) for the reactions of Gibbsite powders with well-stirred sodium hydroxide solutions. ($W_0 = 0.8$ g per 100 cm^3 solution)

T	C (M)	$a_\pm$ (M)	$P11/2$ ($S_0 = 65\,m^2/g$)			$P11/8$ ($S_0 = 32\,m^2/g$)			$P11/48$ ($S_0 = 15\,m^2/g$)			$P11/360$ ($S_0 = 8\,m^2/g$)			$P11/X$ ($S_0 = 5\,m^2/g$)	
			100 k_{w_i}	100 $k_{w_{av}}$	$t_{0.5}$	100 k_{w_i}	100 $k_{w_{av}}$	$t_{0.5}$	100 k_{w_i}	100 $k_{w_{av}}$	$t_{0.5}$	100 k_{w_i}	100 $k_{w_{av}}$	$t_{0.5}$	100 k_w	$t_{0.5}$
20 °C																
	0.25	0.2	40	18	3.8	12.5	7.1	9.7								
	0.5	0.36	75	35	1.9	25	14	4.9	7.8	4.5	15	2.4	1.8	38	0.6	115
	0.75	0.51	110	54	1.3	33	20	3.5								
	1	0.67	140	70	1	40	23	3.3	15	9.2	7.5	5	3.5	20	1.2	58
	1.5	1.07							24	12	5.8	7.6	5.5	12.5		
	2	1.41							30	14	4.9	10	7	10	2.3	30
	3	2.52							45	18	3.8	15	10	6.9	3.3	21
	4	3.65							56	21	3.3	20	13	5.3	4.2	16
	5	5.6										24	16	4.3	6	12
	6	8.1										28	19	3.6	7.2	10
	7	12.3													8.5	8
	8	17.3													10.5	6.5
		1	170		0.9	60		2.2	22		5.5	7		14	2	38
35 °C																
	0.25	0.19	120	58	1.3	58	23	3.3								
	0.5	0.35	220	105	0.67	115	45	1.5	46	23	3.3	13	7.8	8.8	2.6	27
	0.75	0.51	330	175	0.45	170	70	1								
	1	0.68	430	230	0.33	250	90	0.75	90	46	1.5	25	16	4.3	5.2	13
	1.5	1.05							130	70	1	38	23	3	7.5	9.2
	2	1.42							170	85	0.8	50	30	2.3	10.5	6.9
	3	2.42										74	44	1.6	14.5	4.8
	4	3.6										100	56	1.2	18	3.8
	5	5.5													24	2.9
	6	7.8													31	2.2
	7	11.6													50	1.4
	8	16													66	1
		1	600		0.2	340		0.5	130		1.1	46		3.2	7	10
50 °C																
	0.25	0.18										30	13	5.3		
	0.5	0.35										50	25	2.8	9.0	7.7
	0.75	0.51										74	38	1.8		
	1	0.68										100	50	1.4	18	3.8
	1.5	1.02										150	76	0.9	28	2.5
	2	1.35										200	100	0.7	37	1.9
	3	2.31													54	1.3
	4	3.52													70	1
	5	5.2													114	0.6
		1										170		1	25	2.8
65 °C																
	0.25	0.18													25	2.8
	0.5	0.35													49	1.4
	0.75	0.51													75	0.9
	1	0.68													104	0.7
	1.5	1													125	0.55
	2	1.33													175	0.4
	3	2.18													200	0.35
		1													130	0.5

linearly with mean ionic activity upto $a_\pm = 2$–4 g ion/dm^3; then in this range,

$$k_{w_i} = (k_{w_i})_1 \, a_\pm \qquad [5\,\mathrm{B}]$$

k_{w_i} and $(k_{w_i})_1$ values were estimated from eq. [5 A] and [5 B] and are included in the table 2.

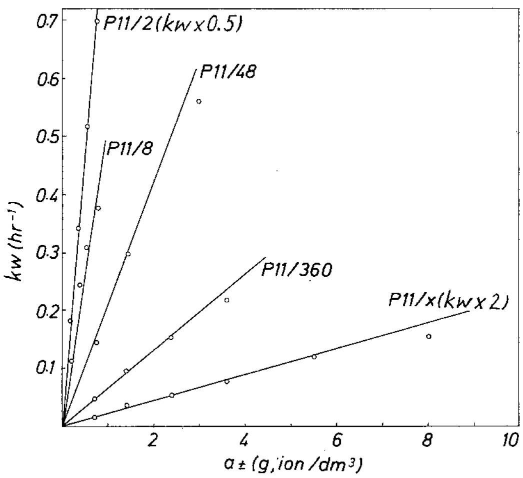

Fig. 5. Dissolution of Gibbsites by sodium hydroxide solutions at 20 °C. Variation of rate constants with mean ionic activity of reaction solution

Powder surface area

Rate constants for dissolution by any hydroxide solution increased markedly with increasing initial surface area of powder. For reactions with any hydroxide solution at any temperature, initial k_{w_i} values for reaction with the high surface area Gibbsite $P\,11/8$ were 25–35 times the k_{w_i} value for reaction with Gibbsite $P\,11/X$; that is, $kk_{wi}^{1/2}$ increased 5–6 times for a 7.5 fold increase in initial surface area. Average $k_{w_{av}}$ values increased 15 to 20 times; that is, $k_{w_{av}}^{1/2}$ increased about 4 times.

Temperature (and energies of activation)

Initial rates of dissolution by any hydroxide solution increased four to five times for a 15 °C rise in temperature. Generally, rate constants increased exponentially with reciprocal absolute temperature; typical $\log k_w - 1/T$ plots are presented in fig. 6. Rate constants of chemically controlled heterogeneous reactions vary, in fact, with temperature according to the relation,

$$k_{w_1} = PZ \exp\left[-E_{\mathrm{act}}/RT\right] \qquad [8]$$

where E_{act} is the energy of activation over the temperature range studied, P, Z are steric and collision factors.

E_{act} values for the reactions studied were estimated using this relation; these were 76, 83, 81, 83, and 83 kg/mole for the dissolution of the powders $P\,11/2$, $P\,11/8$, $P\,11/48$, $P11/360$, and $P11/X$ respectively. These values are all very much lower than the energy required to break open an Al—O bond in an aluminium hydroxide structure.

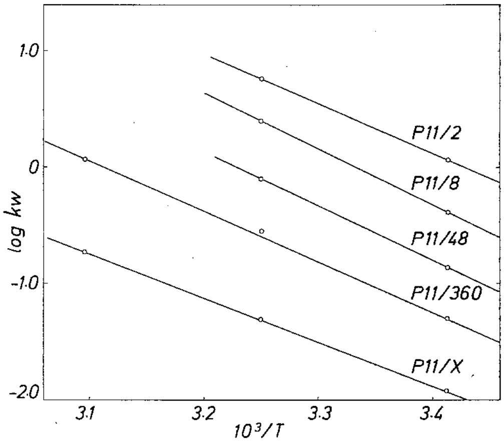

Fig. 6. Dissolution of Gibbsites by sodium hydroxide solution ($C = 1$ M). Variation of rate constants with temperature

Discussion

Dissolution

The experimental studies showed that the dissolution of recrystallised Gibbsite precipitates takes place by a two-directional attack on the six 100 and 110 side faces of the Gibbsite hexagonal platelets; $|\mathrm{Al(OH)_3}|$ layers (18, 19) on the crystal surface dissolve out to form aluminate anions of similar structure (16, 17, 20). The reaction rates at any time depended on the residual weight; this also indicates two-directional dissolution. One-directional dissolution at the two basal hexagon faces would lead to reaction rates independent of powder weight (zero order reactions) while three-directional dissolution would lead to reaction rates depending on $W_t^{2/3}$ or $W_t^{4/3}$ (13).

Rates of reaction and effective surface area

Rates of heterogeneous solid-liquid reactions generally depend on the original effective surface area of the reaction solid and the residual effective surface areas after different times. Effective surface areas may differ significantly from overall surface areas determined by microscopy.

As a working model for the reactions studied in this work, we have considered the two-directional dissolution of a dispersion of W_0 g powder containing N_0 regular hexagonal platelets of initial length l_0 and thickness h. After time t, there would be N_0 platelets of length l_t and thickness h.

Then, the powder weights would be (after times $t = 0, t$),

$$W_0 = \frac{3\sqrt{3}N_0 \varrho l_0^2 h}{8} = 0.65 N_0 l_0^2 h \quad \text{g}$$

$$W_t = \qquad = 0.65 N_0 l_t^2 h \quad \text{g}$$

The surface areas for two-directional dissolution would be

$$A_0 = 6N_0 \frac{l_0}{2} h = 3N_0 l_0 h \quad \text{m}^2$$

$$A_b \qquad = 3N_0 l_t\, h \quad \text{m}^2$$

while the effective surface areas would be

$$A_{\text{effo}} = eA_0 = 3N_0 e l_0 h \quad \text{m}^2$$

$$A_{\text{efft}} = \qquad = 3N_0 e l_t\, h \quad \text{m}^2.$$

Then, the initial specific surface area – for two-directional dissolution is

$$S_0 = A_0/W_0 = 4.6/\varrho l_0 \quad \text{m}^2/\text{g} \qquad [9\text{A}]$$

while the effective specific surface area is

$$S_{\text{effo}} = A_{\text{effo}}/W_0 = 4.6e/\varrho l_0 \quad \text{m}^2/\text{g}. \qquad [9\text{B}]$$

Also,

$$A_0^2 = \frac{9N_0}{0.65\varrho h} W_0 \qquad [10\text{A}]$$

$$A_t^2 = \frac{9N_0}{0.65\varrho h} W_t. \qquad [10\text{B}]$$

Then, eq. [6] may be expressed as

$$\frac{dW}{dt} = -\frac{k_{w_1} W_0}{A^2_{\text{effo}}} A^2_{\text{efft}}\, a_\pm \quad \text{g/h}$$

$$= -k_{a_1} A^2_{\text{efft}}\, a_\pm \quad \text{g/h} \qquad [11]$$

where k_{a_1} is the rate constant w.r.t. effective surface area.

k_{w_1} values in fact depend on k_{a_1} and A_{effo} according to the relation,

$$k_{w_1} = k_{a_1} \frac{A^2_{\text{effo}}}{W_0}. \qquad [12]$$

The initial rate constants for reactions of the Gibbsites P 11/2 to P 11/360 were compared with those for the reactions of Gibbsite P 11/X. According the eq. [12] the ratio

$$r = \frac{k_{w_i}}{(k_{w_i})_x} \quad \text{would equal} \quad \frac{A^2_{\text{effo}}}{(A_{\text{effo}})_x^2} = \frac{S^2_{\text{effo}}}{(S_{\text{effo}})_x^2}.$$

Crystal structure defects and aggregation effects would be minimal for the Gibbsite P 11/X, prepared by prolonged crystallisation; for this material, it was assumed that $(S_{\text{effo}})_x \doteq (S_0)_x$. Then, for the other Gibbsites,

$$S_{\text{effo}} \quad \text{would equal} \quad \sqrt{r}\,(S_0)_x.$$

The effective specific surface areas for the rapid dissolution of the first twenty percent of the high surface area powders were estimated from the above relation: (S_{effo}) values were actually seventy to ninety percent S_0 values, estimated for two-directional dissolution, from crystal lengths.

The effective specific surface areas for the whole dissolutions were about fifty to seventy percent of the S_0 values; the fine powders probably contained appreciable amounts of less reactive aggregated material. Alternatively, preferential adsorption of aluminate anions may retard the reaction with hydroxyl ions during the later stages of reactions.

Reaction mechanism

The results then suggest that the rate of dissolution of the Gibbsites studied is controlled by the rate of a slow reaction,

$|Al(OH)_3| + [OH(H_2O)_2]^-$

surface adsorbed on surface

$\rightarrow [Al(OH)_4(H_2O)_2]^-$

solution

between reactive sites on the crystal surfaces and hydroxyl ions adsorbed on the surface at or adjacent to these sites (13), (21). Then, at any time,

$$dW/dt = -k_{\text{es}} A_{\text{efft}}\, (a_{\text{OH}^-})_{\text{ads}} \quad \text{g/h} \qquad [13]$$

The adsorption of hydroxyl ions on the reactive sites must occur at "low coverage"; then

$$(a_{\text{OH}^-})_{\text{ads}} = bmA_{\text{efft}}\, a_\pm$$

were b is an adsorption coefficient, m is the monolayer adsorption at unit effective surface area.

Thence,

$$dW/dt = -bmk_{es}A^2{}_{\text{efft}}\, a_{\pm} \quad \text{g/h} \qquad [14]$$

$$= -k_{a_1}A^2{}_{\text{efft}}\, a_{\pm} \quad \text{g/h}. \qquad [11]$$

The reactive sites may be at lattice imperfections and dislocations (22) or at electron defect and interstitial Na^+ sites (23); these centres must predominate along planes parallel the "reactive" 100 and 110 faces of the Gibbsite platelets. As the reactive sites at the surface are dissolved out, new reactive sites must be formed and exposed simultaneously until a whole $|Al(OH)_3|$ surface layer dissolves.

Summary

Aluminium hydroxide gels were recrystallised in high pH solution for 2–1000 h to give a series of Gibbsite powders $P\,11/2$, $P\,11/8$, $P\,11/48$, $P\,11/360$ and $P\,11/X$, consisting of hexagonal platelet crystals; their average platelet lengths (l_0) were 0.03, 0.06, 0.13, 0.26 and 0.45 microns. The dissolution of dilute suspensions of these powders in well-stirred sodium hydroxide solutions were studied at 20–65 °C. Reaction solid and solution were analysed after different times by chemical and physical methods.

Reaction occurred by two-directional dissolution of the platelet crystals. The reactions of Gibbsite $P\,11/X$ (prepared by prolonged 1000 h crystallisation) were first order w.r.t. powder weight (and second order w.r.t. powder effective surface area); the reactions of the other Gibbsites were first order for the first twenty percent rapid dissolution and then slower. The initial rate constants k_{w_1} (h^{-1}) and half-lifes $t_{0.5}$ (h) for reactions of $P\,11/2$, $P\,11/8$, $P\,11/48$. $P\,11/360$ and $P\,11/X$ with sodium hydroxide solution of unit mean ionic activity at 20 °C were 1.70, 0.9; 0.60, 2.2; 0.22, 5.5; 0.07, 14 and 0.02, 38 respectively.

Rate constants increased linearly with the mean ionic activity of the hydroxide solution and increased exponentially with reciprocal absolute temperature, four to five times for 15 °C temperature rise. Half-lifes decreased in a similar manner. Energies of activation varied from 76–83 kJ/mol. The rates of dissolution are determined by the rate of the chemical reaction between adsorbed hydroxyl ions and adjacent reactive aluminium hydroxide sites on the powder crystal surface.

Zusammenfassung

Aluminiumhydroxydgele werden in Lösungen höher pH 2 bis 1000 Std. rekristallisiert und ergeben dabei eine Reihe von Gibbsit-Pulver $P\,11/2$, $P\,11/8$, $P\,11/48$, $P\,11/360$ und $P\,11/X$. Sie bestehen aus hexagonalen plättchenförmigen Kristallen. Die mittlere Dimension (l_0) waren 0,03; 0,06; 0,13; 0,26 und 0,45 microns. Die Auflösung von verdünnten Suspensionen dieser Pulver wurden in stark gerührten Natriumhydroxyd-Lösungen bei 20 bis 65 °C untersucht. Das feste Reaktionsprodukt und die Lösung wurden nach verschiedenen Zeiten mit chemischen und physikalischen Methoden analysiert.

Die Reaktion erfolgte durch zwei-dimensionale Auflösung der Blättchen. Die Reaktion von Gibbsit $P\,11/X$ (präpariert durch eine auf 1000 Std. verlängerte Kristallisation) waren von 1. Ordnung hinsichtlich Pulvergewicht, und von 2. Ordnung hinsichtlich effektiver Oberfläche. Die Reaktion der anderen Gibbsite waren von 1. Ordnung für die ersten 20% schnelle Lösung und wurden dann langsamer. Die anfänglichen Reaktionskonstanten und Halbzeiten der Auflösung für alle Gibbsite in Natriumhydroxyd-Lösungen der Ionenstärke 1 waren 1,70; 0,9; 0,60; 2,2; 0,22; 5,5; 0,07; 14 und 0,02, 38. Zahlen in der Reihenfolge $P\,11/2$ bis $P\,11/X$.

Die Geschwindigkeitskonstanten wachsen linear mit der mittleren Ionenaktivität der Hydroxylödung und wachsen exponentiell mit der reziproken absoluten Temperatur auf das Vier- oder Fünffache für 15 °C Temperaturanstieg. Die Halblebensdauern nehmen in analoger Weise ab. Die Aktivierungsenergien variieren zwischen 76 und 83 kJ/mol. Die Geschwindigkeiten der Auflösungen werden durch die Geschwindigkeit der chemischen Reaktion bestimmt. Zwischen den adsorbierten Hydroxyd-Ionen und den anhaftenden reaktiven Aluminiumhydroxydplätzen an der Kristall-Pulver-Oberfläche.

References

1) *Willstaetter, R.*, Berichte **57B**, 1082 (1926).

2) *Weiser, H. B.*, Advances in Colloid Science, Part I, 227 (1942).

3) *Bye, G. C.*, Kolloid-Z. u. Z. Polymere **198**, 53 (1964).

4) *Packter, A.* and *H. S. Dhillon*, Kolloid-Z. u. Z. Polymere **239**, 598 (1970).

5) *Souza Santos, P.*, Kolloid-Z. **133**, 101 (1953).

6) *Vogel, A. I.*, Quantitative Inorganic Analysis, Chap. **4**, 436; Ch. **14**, 885 (Harlow 1962).

7) *Waenninen, E.*, Anal. Chem. Acta, **12**, 308 (1955).

8) *Klug*, H. P. and *C. E. Alexander*, X-ray Diffraction Procedures, Chap. **7** (New York 1954).

9) *Frederickson, L. D.*, Anal. Chem. **26**, 1883 (1955).

10) *Torkar, K.*, Monatsh. (Wien) **92**, 512 (1961).

11) *Kay, D. H.*, "Techniques of Electron Microscopy", Chap. 3 (Oxford 1965).

12) *Åckerlof, G.*, J. Amer. Chem. Soc. **59**, 1855 (1937).

13A) *Packter, A.* and *H. S. Dhillon*, J. Chem. Soc. **A 1969**, 2588 (1969).

13B) *Dhillon, H. S.*, Ph. D. Thesis, London University (1971).

14) *King, C. V.*, J. Amer. Chem. Soc. **68**, 238 (1946).

15) *Harriott, P.*, A. I. Chem. Eng. J. **8**, 93 (1962).

16) *Pearson, T. G.*, R. I. C. Monograph **3** (1955).

17) *Brossett, C.*, Acta Chem. Scand. **8**, 1917 (1954).

18) *Deer, W. A.*, Rock-forming Minerals, Vol. **5**, 93 (Harlow 1965).

19) *Megaw, H. D.*, Z. Kristall. **87**, 185 (1934).

20) *Hem, J. D.*, Advances in Chemistry Series (U.S. Geological Survey), **73**, 98 (1968).

21) *Granquist, W. T.*, Proc. 6th National Conf. Clays 293 (1959).

22) *van Bueren, H. G.*, "Imperfections in Crystals", Chap. **3**, 4 (Amsterdam 1960).

23) *Gregg, S. J.*, J. C. S. 3804 (1955).

Authors' address:

A. Packter and *H. S. Dhillon*
Chemistry Department
N.E. London Polytechnic
London E 15 (England)